Smart Grids and Sustainable Energy (2023) 8:18
https://doi.org/10.1007/s40866-023-00177-y

ORIGINAL PAPER

ASS-MPPT and 2TSO Algorithm-Based Design and Evaluation of a Wind-Biomass Hybrid Power Generation Systems

Subhadip Goswami[1] · Tapas Kumar Benia[1] · Abhik Banerjee[1]

Received: 11 August 2023 / Accepted: 20 October 2023 / Published online: 6 November 2023

Abstract

The utilization of conventional sources augments the demand for energy, thus resulting in the usage of Renewable Energy Sources (RESs). It is convenient to add another energy source to solar along with wind energy sources since these RESs could not be tapped continuously. Fulfilling the electric load demands with higher unpredictability might not be practical with stand-alone energy systems. Thus, to overcome the stand-alone energy systems' weaknesses, it would be highly significant to amalgamate one or more energy systems. To provide expanded system effectiveness together with a greater balance in power supply, generally, two or more energy sources are comprised in a Hybrid Renewable Energy System (HRES). To produce electricity, the energy from wind and biomass is utilized in the proposed methodology. The rectifier is utilized with the inverter since the inverter operates with the DC input source. The Adjustable Step Size Maximum Power Point Tracking (ASS-MPPT), which regulates the output voltage by tuning the pulse width, is deployed in the inverter to attain a response for power control. By amalgamating the generation energy from wind as well as biomass systems, a Hybrid Power Generation System (HPGS) has been proposed. In the experimental evaluation, the technical feasibility of incorporating wind along with biomass systems for the needed demand has been analyzed. The experiential outcomes proved that to gratify the energy demands, higher efficiency could be delivered by the proposed hybrid system.

Keywords Wind energy · Biomass · Taxicab Tunicate Swarm Optimization (2TSO) · Adjustable Step Size Maximum Power Point Tracking (ASS-MPPT) · Hybrid power generation system

Introduction

Globally, the electrical power supply has turned into one of the most vibrant source requirements in recent days. The energy sources' capacity, which would have doubled over the coming 40 years, was installed by the World Bank and International Energy Agency (IEA) to fulfil the energy demands [1, 2]. The IEA, which renders policy recommendations, analysis, along with data on the whole global energy sector, is a Paris-centric autonomous intergovernmental organization, established in 1974. 75% of global energy demand is represented by the 31 member countries and 13 association countries of the IEA. The fundamental concept of the IEA is to scale up action on energy efficiency for mitigating climate change, improving energy security, and growing economies while delivering environmental and social benefits. Energy consumption has increased owing to the augmentation in the demand for electricity in office complexes, industries, institutions, commercial establishments, et cetera. In today's situation, it is highly required to abate the greenhouse gas emissions from conventional thermal power plants [3]. On the whole world, such emissions bring about hazardous consequences of climate change to electricity producers. Therefore, presently, the world is moving towards RESs on a larger scale to safeguard the environment and support sustainable development [4–7]. As per human standards, the RES is inexhaustible; in addition, it has the need for fossil fuels for electricity requirements and for mitigating the greenhouse gas emissions level [8]. Here, approximately 75% of fossil fuels were utilized for fulfilling the current world energy demand [9]. Next, with environmentally friendly, sustainable, and renewable resources, a more energy-efficient economy could be developed to satisfy the higher electricity demand; here, wind, biomass, solar, geothermal, tidal,

✉ Subhadip Goswami
subhadipgoswami1@outlook.com

[1] Department of Electrical Engineering, National Institute of Technology, Arunachal Pradesh, Itanagar, India

and biofuel are the renewable resources utilized as different energy sources [10, 11]. Amongst these biomass, solar, and wind power generation are deemed to be the capable technologies since, instead of utilizing conventional power, they operate thermally driven power generation systems; moreover, the only RES that releases carbon dioxide (CO2) in usage is biomass [12].

The conversion of energy from sunlight into electricity is termed solar power; here, the electricity is formed either by directly utilizing the Photovoltaic (PV), by indirectly utilizing concentrated solar power, or by the amalgamation of both. Similarly, the usage of air flow via Wind Turbines (WTs) is termed wind power; here, the wind energy is extracted by the turbine, which then generates the mechanical power to start the electric generators; during this operation, no greenhouse gas is emitted. Moreover, merely little land is needed for this and it utilizes no water; in addition, the non-hydro global renewable energy's biggest part is comprised here with 514 GW capacity. The wind farm converts kinetic energy into AC power by utilizing the rectifier; then, it is transmuted into DC power [13–15]. During low as well as non-sunshine hours, biomass is deemed to be the best option for partial along with full load energy needs; additionally, they supplement every single other occasionally. It is a carbon-centric fuel developed as of organic material. Agricultural residues, animal wastes, forestry, Municipal Solid Waste (MSW), et cetera are the various sorts of biomass [8 and 16]. To reduce the electricity cost whilst augmenting the dispatch-ability in operation, hybrid power generation is regarded as a highly promising operational requirement owing to its intermittent nature together with the unpredictable power output of renewable sources like biomass, wind, and solar power [16–18]. Nevertheless, the environment could be harmed whilst manufacturing solar panels; thus, wind and biomass are the most promising requirements. In this, better reliability with energy storage is provided by the hybrid generation; also, it provides lower-cost energy [19]. The hybrid power generation systems are reliable; also, they satisfy the load demand very closely in all seasons since in this proposed work, the hybrid power generation system is developed grounded on the sources of wind and biomass. Even in windless weather with high power demand, biomass can continuously generate the electricity because biomass-based electricity generation is climate-friendly.

Consequently, owing to the power generated by solar along with wind power plants, which substitute the power from conventional units (because of priority dispatch as well as lower marginal cost), the renewable generation sources could not provide a specific amount of power. Thus, by amalgamating wind along with biomass, an Adjustable Step Size MPPT (ASS-MPPT) and Taxicab Tunicate Swarm Optimization (2TSO)-centric HPGS have been proposed here. In addition, the factors that contribute to the hybrid power generation system for increased system efficiency as well as greater balance in energy supply are listed below.

- An effective inverter control unit is proposed for monitoring and tracking maximum power points.
- An ASS-MPPT is employed in the proposed research to regulate the output power to the load by altering the pulse width in the modulation scheme.
- An efficient TSO technique is employed in a hybrid system to attain better performance.
- A low-cost system design is proposed to produce continuous power generation under fluctuating atmospheric conditions.

The paper's remaining parts are organized as: the related works concerning the proposed framework are reviewed in Section "Related works"; the proposed mechanism is detailed in Section "Proposed hybrid power generation system"; regarding certain performance metrics, the outcomes along with discussion are exemplified in Section "Result and discussion"; lastly, the paper is wrapped up in Section "Conclusion".

Related works

Ling Ji et al. [20] developed the mixed-integer programming optimization system; this model mainly concentrated on the total minimum annualized cost of the techno-economic analysis of the stand-alone Hybrid Energy System (HES) along with the optimal design for the typical rural village in northwest China. A Levelized Cost of Energy (LCOE) consumption along with the LCOE production was utilized to analyze the economic cost of energy; accordingly, analyzed the economic COE as of supply together with the demand side. The outcomes demonstrated that in the most economical option of PV/ biomass-CHP/diesel generator/gas boiler/ battery/thermal energy storage HES, the model attained 652 103 $ of total annualized cost. Moreover, when compared with the energy consumption (0.275 $/kWh), the LCOE consumption (0.355 $/kWh) was high; thus, implying a highly flexible heat/power output equipment as well as greater potential meant for local electrification. Nevertheless, owing to the expensive capital cost, the model's cost was higher.

H. El-houari et al. [21] recommended the amalgamation of standalone HRES to provide a continuous power supply. The experimentation was conducted in 10 houses that were positioned in the remote village of Tazouta positioned in the Moroccan Fez-Meknes province. When analogized to the grid extension along with the traditional diesel generator, the CO2 equivalent greenhouse-gas emission was mitigated up to 26.48 tons annually with the methodology having 100% renewable energy penetration. Moreover, it was revealed that in the energy cost of the optimum configuration in PV Wind-Biomass-Battery, the average energy requirement of 91.38 kWh/day along with a peak load of 6.44Kw and 0.2 \$/kWh was established; additionally, no non-RES was enclosed in the presented model. However, the model was adopted only in a specific area; thus, accurate outcomes could not be attained.

Mohammad Hossein Jahangir and RaminCheraghi [22] concentrated on the HES comprising PV panels, WTs, and Biogas Generator (BG) for rural electrification in Fars province in Iran. For the development of fossil fuel power plants along with CO2 emissions of the exploitation of that off-grid system, the presented model was utilized. The emission of harmful gases together with the dependence on fossil fuels was mitigated by the off-grid system. The Hybrid Optimization Model for Electric Renewable (HOMER) Pro software was utilized to address the optimization problem. The outcome demonstrated that in optimal systems, the Cost of Electricity (COE) ranged from 0.128 to \$0.223/kWh. When the biomass price increased as of 20 to \$60/ton, the BG's power generation was mitigated by up to 86%. Additionally, PV panels (80.7 kW), a BG (150 kW), batteries, and a converter were included in the optimal economic system. However, when analogized with the coal-centric power plant along with the grid, the CO2 emissions from the HRES were trifled.

Loiy Al-Ghussain et al. [23] adopted the Generalized Reduced Gradient algorithm, which was wielded to analyze the optimal components' capacities in PV/wind/biomass hybrid systems with as well as devoid of energy storage made regarding maximized Demand–Supply Fraction (DSF) along with the Renewable Energy Fraction (REF) with a net present value greater than or equivalent to zero. The model subsumed 1.79 MW PV, 2 MW wind, along with 0.92 MW biomass system with 24.39 MW and 148.64 kWh batteries that attained REF of 99.59%, the COE equivalent to 0.1626 \$/kWh, along with 98.86% of DSF. The outcomes demonstrated that almost 99% of autonomy was obtained by the incorporation of a hybrid energy storage system with the PV/wind/biomass system. However, here, the time complexity was high.

S.K.A. Shezan and H.W. Ping [24] presented a PV-wind-biomass-diesel battery HES to offer the power supply to an off-grid community for the problems in shipping fossil fuel supply to the remote territories in northern islands near the Bay of Bengal of Bangladesh. In this model, the CO2 emission was mitigated by about 1600 tons (29.65% per annum). Finally, it was evident that the optimized system's COE was about USD 0.431/kWh; similarly, its Net Present Cost (NPC) was about USD 160,626.00. Then, the methodology was analogized with the mixture of routine vitality frameworks; moreover, it was very expensive.

Proposed Hybrid Power Generation System

To offer better system efficiency together with a higher balance in energy supply, the HPGS is highly essential. From RESs like PV panels, wind, or smaller hydro turbines, two or more energy sources are amalgamated in a typical hybrid system. Here, this paper proposed an ASS-MPPT as well as 2TSO-guided HPGS, which amalgamates the energy sources of wind together with biomass. A WT system, three-phase bridge rectifier, biomass system, inverter control unit, and grid system are included in the proposed methodology. Figure 1 exhibits the proposed model's block diagram.

Wind Energy

The utilization of WTsto produce electricity as of the wind force is termed wind energy. By the use of wind turbines, wind could be utilized to make electricity. Wind turbines are taller structures that contain larger blades, which rotate when the wind blows. As the blades turn, they spin a shaft that is connected to a generator. A wind turbine's blades are made for collecting the wind's kinetic energy. The wind exerts pressure on the blades, turning them. The blades' angle and shape are specifically chosen to maximize the quantity of wind energy that can be harvested. More energy may be gathered as the wind blows faster. A wind turbine's generator is similar to the one in a conventional power plant. It comprises a number of magnetically encircled wire coils in a series. The wind turbine's shaft rotates, spinning the coils of wire inside the magnetic field. In turn, the electrical grid can receive this current, which is produced in the cables. The wind speed is not a constant value; it alters hourly as well as seasonally. The maximum power generated by the WT regarding the time performance is expressed as follows,

$$\omega_{\text{wind}} = \begin{cases} \omega_{RP} \frac{\vartheta - \vartheta_{ci}}{\vartheta_{RS} - \vartheta_{ci}} & \vartheta_{ci} < \vartheta < \vartheta_{RS} \\ \omega_{RP} & \vartheta_{RS} < \vartheta < \vartheta_{co} \\ 0 & \vartheta \le \vartheta_{ci} \text{or} \vartheta \ge \vartheta_{co} \end{cases} \tag{1}$$

where, the model's rated power is specified as ω_{RP}, the rated speed is signified as ϑ_{RS}, and the cut-in and cut-off speeds are represented as ϑ_{ci},ϑ_{co}. The energy extracted by the wind turbine blades $\left(\varpi_{tb}\right)$ is formulated as,

$$\varpi_{tb} = \frac{\eta_b a_{SA} \rho_{ad} \vartheta^3}{2} \tag{2}$$

where, the swept area is notated as a_{SA}, the air density is symbolized as ρ_{ad}, and the average wind speed is indicated as ϑ.

Biomass Energy

From plants as well as animals, the renewable energy generated is termed biomass. Energy resources and recycling along with the usage of waste are offered by the unused biomass. The major source of producing electricity is biomass combustion, which could be obtained via

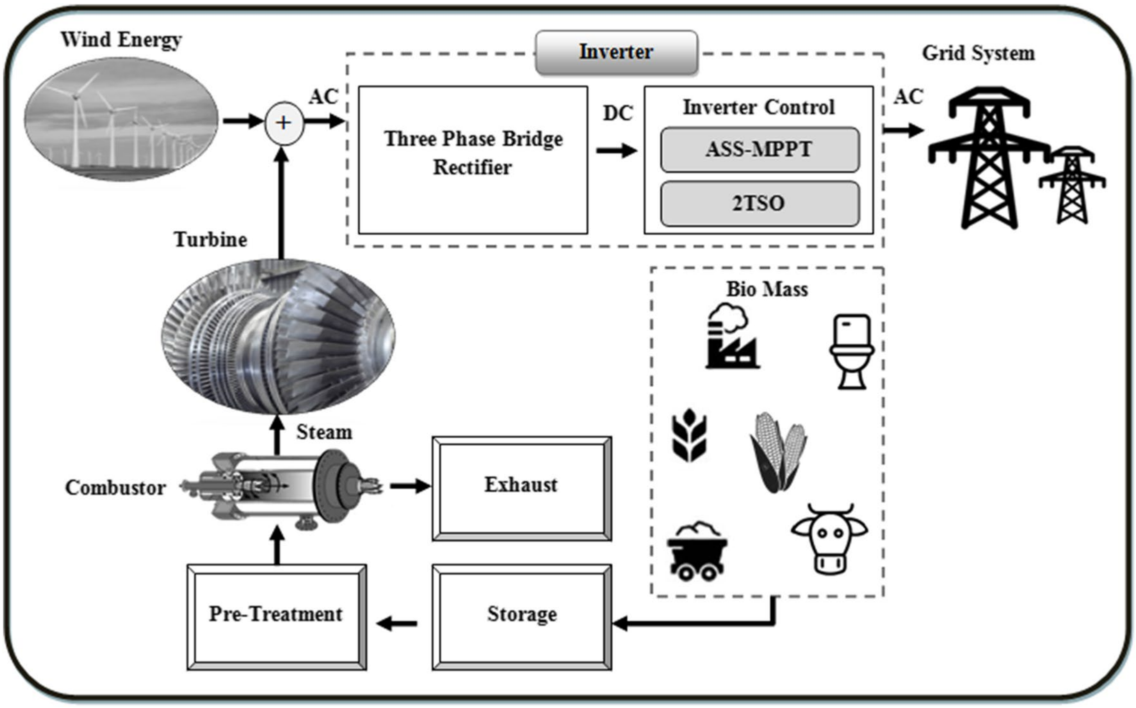

Fig. 1 Block diagram of the proposed system

biogasification. Moreover, biomass acts as a popular alternative to fossil fuels because it has a lower environmental impact andcould be replaced quickly (times ranging from 1 growing season to perhaps 1 or else 2 decades) devoid of permanently depleting Earth's natural resources. Comparatively, it takes millions of years to generate fossil fuels like coal, petroleum, and natural gas.For the rural environment biogas, for the energy demands, a product from biomass is considered to be a unique solution. Initially, the biomass is stored. Next, for certain biomass waste, pre-processing is performed. Then, to generate hot gas, the biomass is burned in the combustor directly; the gas being generated is provided to the boiler to produce steam, which is then inputted into a steam turbine to generate mechanical energy.

Combustor Burning biomass in such a way that it offers a higher stagnation temperature with smaller losses in stagnation pressure along with lower pollution emissions is the vital function of the combustor. To turn the power turbine, the higher-temperature exhaust gas obtained is utilized; thus, producing thrust.In simple terms, a power turbine works by utilizing a heat source to heat water to extremely high temperatures until it is converted into gas. As that steam flows passed a turbine's spinning blades, the steam expands and cools. A higher exhaust temperature could result in overstressing turbine blades since as temperature increases, the strength of gas decreases. Therefore, the higher temperature is utilized here.

Turbine To generate electricity via movement, a turbine, a steam-powered machine, is utilized.The turbine generator comprises steam of moving fluids likecombustion gases. the stator blades in the steam turbines accelerate and swirl higher-temperature as well as higher-pressure steam provided from their boilers around the rotor. Afterward, impulse forces and reaction forces are received from the accelerated and swirled steam by the rotating blades. After that, the torque is transmitted by the rotating blades to the rotors produced by the steam forces. The generator's rotor shaft is spun/rotated by the force of the fluid on the blades. Then, the generator converts the rotational energy from the shaft into electrical energy.Via the series of turbine blades, the steam generated by combustion flows; subsequently, the electrical energy is produced by the rotation of the turbine. The biomass from the biogas $\left(B_{tb}\right)$ is measured as,

$$B_{tb} = \sum_{k=1}^{K} \phi_{L(k)} J_{\phi(k)} \delta_J \Theta_J \sigma_B \hbar_B \tag{3}$$

where, the specified groups of living population in particular regions is indicated as $\phi_{L(k)}$, the manure produced per one individual $\phi_{L(k)}$ in a year is denoted as $J_{\phi(k)}$, the dry matter content as of $J_{\phi(k)}$ is depicted as δ_J, the manure's organic matter is signified as Θ_J, the biogas volume is indicated as

σ_B, and the heat energy content from the biogas is notated as $\hbar_B$. The mechanical energy from WTs $\left(\varpi_{tb}\right)$ along with biomass steam turbines $\left(B_{tb}\right)$ is provided to the three-phase bridge rectifier.

Three-Phase Bridge Rectifiers

A solid-state semiconductor device is subsumed in a three-phase rectifier; this device is an electronic component in which to perform the rectification, the current is passed only in a forward direction. Three-phase rectifier delivered a large amount of power to the load. Its efficiency is high. The ripple factor is less. It does not require an additional filter.The process of transmuting the AC input supply into a fixed DC supply is termed rectification. Figure 2 exhibits the three-phase rectifier's circuit diagram.

As shown in Fig. 2, betwixt the first and second phases, the bridge rectifier network is formed by the diodes 1, 2, 3, and 4; likewise, betwixt the second and third phases, the network is formed by the diodes 3, 4, 5, and 6; eventually, betwixt the third and first phases, the network is formed by the diodes 1, 2, 5, and 6. The positive rail is fed by diodes 1, 3, and 5; here, the diode, which has a larger positive voltage at its anode terminal, conducts. Likewise, the positive rail is fed by diodes 2, 4, and 6; in this, the diode conducts when it has a larger negative voltage at its cathode terminal. The 6 segments within 1 fundamental source period correspond to the various line-to-line source voltage combinations (V_{LL}). A minimum along with maximum DC voltage is present in every single segment:The minimum along with DC voltage could be obtained in accordance with the line-to-line source voltage combinations. Minimum DC voltage: the DC voltage will be at a minimum of $V_{DC} = V_{LL} \cdot \sin(60°)$if one line-to-line voltage is zero.Maximum DC voltage: The DC voltage increases up to a maximum of $V_{DC} = V_{LL}$ in which 2 line-to-line voltages are equivalent.The DC voltage's average value that lies betwixt the minimum and maximum voltage could be formulated as,

$$V_{\mathrm{out}(dc)} = \frac{3}{\pi} \int_{\frac{\pi}{3}}^{\frac{2\pi}{3}} \sqrt{3} V_m \sin\theta \, d\theta \tag{4}$$

where, the output DC voltage across the load is specified as $V_{\mathrm{out}(dc)}$, and the line voltage relying on which the diode pairs conducting is signified as V_m. The output voltage's RMS value is denoted as,

$$V_{rms(\mathrm{out})} = \sqrt{\frac{9}{\pi} \int_{\frac{\pi}{3}}^{\frac{2\pi}{3}} \left(V_m \sin\theta\right)^2 d\,\theta} \tag{5}$$

The output voltage is lesser than the line voltage or it is 2.34 times the RMS phase voltage $V_{rms(\mathrm{out})}$.

Inverter Control

From the rectifier, the DC output voltage is taken by the inverter; then, by utilizing the sinusoidal Pulse Width Modulator (PWM), it alters the transmuted DC back into AC.PWM control for induction motors is a technique used to control the speed or torque of an induction motor by varying the width of pulses in a square wave signal. It is a widely used method for motor control due to its simplicity and effectiveness.One of the most significant efficacies of the PWM is that it generates a pure sine wave signal with lesser harmonic distortion. Therefore, owing to the diminished harmonics related to the pure sine wave shape, inductive loads like motors start easier and run cooler.Also, the sine wave reduces the audible and electrical noise when utilized in the appliances. The DC/AC conversion mechanism switches power transistors, namely "IGBT (Insulated Gate Bipolar Transistor)" and changes the ON/OFF intervals for creating

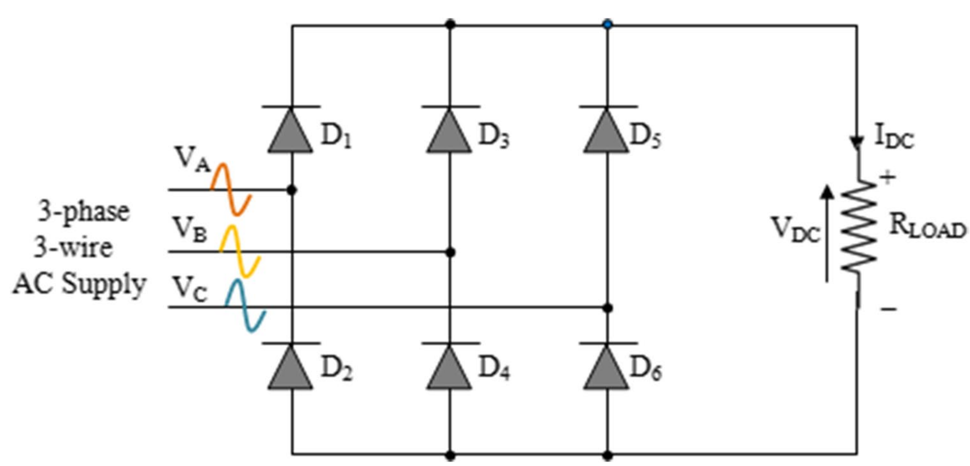

Fig. 2 Three-Phase Bridge Rectifier

pulse waves with various widths.The duty cycle, which is the ratio of on-time to the total period, determines the average voltage applied to the motor windings. By changing the duty cycle, the effective voltage and the motor speed or torque could be controlled.These pulses are then filtered and smoothed by capacitors and inductors to form a sinusoidal waveform, which is the most common type of AC.It then integrates them into a pseudo-sine wave. This is named "Pulse Width Modulation (PWM)".To stabilize the voltage regulation, the PWM charge controllers need the battery's voltage as a reference. Adjustable Step Size MPPT (ASS-MPPT) is utilized in the proposed research to regulate the output power to the load by altering the pulse width (i.e., duty cycle) in the modulation scheme.

Adjustable step size MPPT

In power systems, MPPT techniques are engendered to increase efficacy. Various algorithms have been developed in MPPT; amongst those techniques, owing to its effortless implementation, Perturb and Observe (P&O) is utilized extensively. For extracting maximum power from the inverter and delivering it to the load, the P&O algorithm is utilized. The proposed MPPT technique transfers the maximum power from the PV source to the load or grid by adjusting theDC-DC converter's duty cycle under variable weather conditions. In the conventional P&O technique, temperature, light intensity, along with other external environment elements are assumed to be constant;a small perturbation is applied to theinverter's voltage or current;the working point's output voltage and current before and after the perturbation is detected; also, the corresponding power is computed. The current working point is judged by observing the power changes of these two working points. The perturbation will be applied in theprevious perturbation's direction if the power increases. If the power decreases, the perturbation will be applied in theprevious perturbation's opposite direction until the working point finally approaches the maximum power point.MPP tracking speed is faster in fixed step sizewhen the step size is kept larger with larger oscillations around MPP, which means a loss in power. Conversely, the steady-state oscillation will be greatly reduced by a small fixed step at the cost of a slower response. Simultaneously, it has the tendency to fail in MPPT within the condition of swiftly altering atmospheric situations along with a lack of source. Therefore, to attain the MPP, which is gauged by utilizing the Taxicab Tunicate Swarm Optimization (2TSO) algorithm, rather than utilizing the fixed step size, an ASS is adopted in the proposed methodology. ASS tracks MPP faster and runs near MPP with very small fluctuations.The oscillations around the MPP are reduced by varying thestep size value, thus resulting in a faster response for reaching it. If the operating point is far from the MPP, it increases the step size, thusenabling a faster tracking capability. Here, the duty cycle is varied as a sine wave in addition to controlling the power by altering the modulation index. It is formulated as,

$$dc = \varphi sin\ \varpi t \tag{6}$$

where, the duty cycle is denoted as dc, and the modulation index is specified as φ. The P&O algorithm works under 2 conditions, which are,

- If an elevation in voltage brings about an increase in power, then the operating point moves in that direction by augmenting the modulation index as, $\varphi = \varphi + \updownarrow_{adj}$.
- If an increase in voltage brings about an augmentation in power, then the operating point is in the opposite direction by mitigating the modulation index as $\varphi = \varphi - \updownarrow_{adj}$.

Until the derivative of power regarding voltage is equivalent to zero, the algorithm continues perturbations. Figure 3 demonstrates the pseudo-code of the proposed ASS-MPPT algorithm.

By utilizing the 2TSO algorithm, the ASS $\updownarrow_{adj}$, which mitigates the instantaneous error betwixt the reference and the actual current, is computed to enhance the controller tracking.

Computing Step Size Via 2TSO

Tunicate Swarm Optimization (TSO), a simple meta-heuristic optimizer, imitates the tunicates' natural foraging process, particularly, their swarming behaviour along with their jet propulsion during navigation. To locate food sources in the sea, the tunicate swarms. In this swarming, based on the first best tunicate, the tunicates update their position; moreover, the positions being updated are accumulated as well as upgraded in every single iteration. (i) Should avoid collision with other tunicates, (ii) should take the correct path to the optimal search space, and (iii) should be close to the best search agent are the 3 significant criteria that must be satisfied by the tunicates during navigation. Migrating tunicates vertically is possible in the ocean with propulsion. The distance betwixt a food source and search agent is computed as the difference betwixt them in the traditional TSO algorithm; in addition, a random number is multiplied by the search agent. However, it is not effective; thus, the convergence is extremely slow. The ineffective performance and slow convergence are obtained by the inclusion of random numbers,which restricts to provide optimal value to reach the best neighbour.Hence, the current search agent does not move towards the best position. Therefore,the number of iterations is increased.Thus, the computation time of

Fig. 3 Pseudo-code of the ASS-MPPT algorithm

```
Input: current and voltage V_dc, I_dc
Output: maximum power

Begin
    Initialize parameters, number of iterations I_max
    While (I < I_max) do
    Set modulation index φ
    Measure V_dc, I_dc
    Compute power p
        If (P_new > P_old) {
            If (V_dc(new) > V_dc(old))
                Increase modulation index φ = φ + ℓ_adj
            Else
                Decrease modulation index φ = φ − ℓ_adj
        } End if
        If (P_new < P_old) {
            If (V_dc(new) > V_dc(old))
                Decrease modulation index φ = φ − ℓ_adj
            Else
                Increase modulation index φ = φ + ℓ_adj
        } End if
End
```

step size is increased.For distance computation, the Taxicab Metric is utilized, also, in the updation phase, velocity computation is performed to overcome the drawback. This significantly eliminates the uncertainty caused by randomness and reduces the moving complexity. Therefore, the number of iterations can be reduced with optimal computation of step size. Also, it converged quickly.

In this proposed algorithm, the tunicates must keep migrating toward their best search agent to prevent conflict in the first place. Finally, they must stay close to that agent. The other tunicates in the mathematical model employ swarm intelligence to update their positions in relation to the ideal solution.

Initially, the reference currents areassumed as the number of tunicates, and the actual current levels are considered as the foods.

Avoiding collision The new search agent's position is measured to deter collision betwixt the search agents whilst searching for a better position.The tunicates' random positions along with constant parameters are initialized as,

$$\vec{D} = \vec{W} * \frac{1}{\vec{F}} \tag{7}$$

$$\vec{W} = \kappa_2 + \kappa_3 - \vec{R} \tag{8}$$

$$\vec{R} = \kappa_1 . \vec{R} \tag{9}$$

$$\vec{F} = \left[f_{\min} + \kappa_1 \left(f_{\max} - f_{\min} \right) \right] \tag{10}$$

where, the new agent's position vector is specified as $\vec{D}$, the gravity force is signified as $\vec{W}$, the new vector to store the social forces betwixt agents is denoted as $\vec{F}$, the water flow in the deep ocean is indicated as $\vec{R}$, the three random numbers are notated as κ_1, κ_2, and κ_3, and the initial, as well as subordinate speeds to make social interaction, are symbolized as $f_{\min}$,$f_{\max}$.Regarding the instantaneous error, the fitness is analyzed after initializing the position.

Moving Toward best Neighbour

To reach an optimal solution, the search agents move towards the best neighbour's direction when no collision transpires betwixt the neighbours.The finest neighbour's position (i.e., food source) is formulated as,

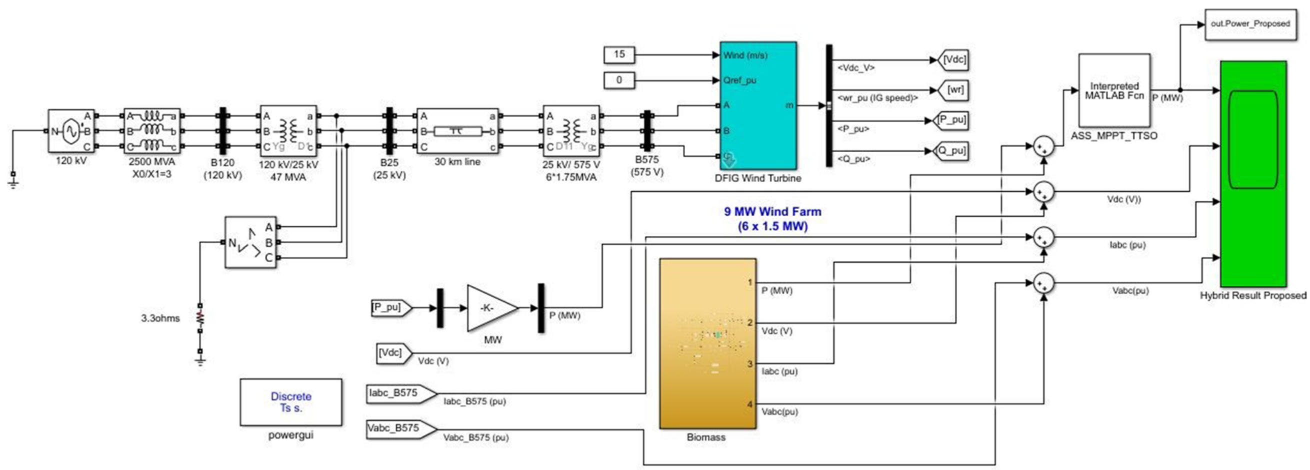

Fig. 4 Simulation of the proposed method

$$d_{A,S} = \mid Z_{\text{best}(m)} - Z_{\text{best}(m+1)} \mid + \mid Z_{A(m)} - Z_{A(m+1)} \mid \tag{11}$$

where, the taxicab distance betwixt search agent and food source is notated as $d_{A,S}$, the search agent's best position is specified as $Z_{\text{best}(S)}$, the position of tunicates at current iteration m is symbolized as Z_A, the random number is represented as $\varepsilon \in (0, 1)$, and the positions of the first two tunicates are indicated as $Z_{\text{best}(m+1)}$,$Z_{A(m+1)}$.

Remains close to the best search agent The search agent could retain its position towards the best search agent. The tunicates' position could be updated as in the following equation to ensure that the search agent is still close to the best agent.

$$Z_{A(m)} = \begin{cases} Z_{\text{best}(S)} + \vec{D}.d_{A,S} & \text{if } (\varepsilon \geq 0.5) \\ Z_{\text{best}(S)} - \vec{D}.d_{A,S} & \text{if } (\varepsilon < 0.5) \end{cases} \tag{12}$$

where, the updated position of tunicates regarding the best position $Z_{\text{best}(S)}$ is signified as $Z_{A(m)}$. For mathematically simulating thetunicate's swarm behavior, the first 2 optimal best solutions are saved, and the other search agents' positionsare updated as per the best search agents' position. For defining the tunicate's swarm behavior, the formula is given as:

$$Z_{A(m+1)} = \frac{Z_{A(m)} + Z_{A(m+1)}}{2 + \kappa_1} \tag{13}$$

For the updated position, the fitness is evaluated; subsequently, the position is updated by utilizing $Z_{A(m+1)}$ when a better solution occurs. The final position will be in a random place, within a cylindrical or else cone-shaped, which is described by the tunicate's position. As the tunicates found their food sources the optimal step size is gauged by utilizing the 2TSO methodology; in addition, it is updated to the inverter controller.

Table 1 Analysis of wind speed

Month	Speed (m/s)
January	3.2513
February	3.4517
March	3.8527
April	3.7926
May	3.6738
June	3.7717
July	3.5416
August	3.4756
September	2.8939
October	2.8926
November	3.1926
December	3.1216

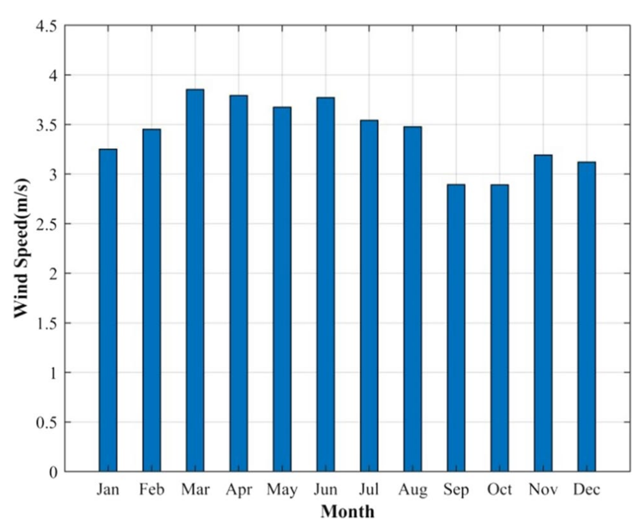

Fig. 5 Graphical representation of wind speed

Table 2 Analysis of wind and biomass power

Month	Wind power (kW)	Biomass power (kW)
January	200	1300
February	380	1120
March	400	1100
April	800	700
May	250	1250
June	900	600
July	1100	400
August	350	1150
September	1450	50
October	250	1250
November	200	1300
December	220	1280

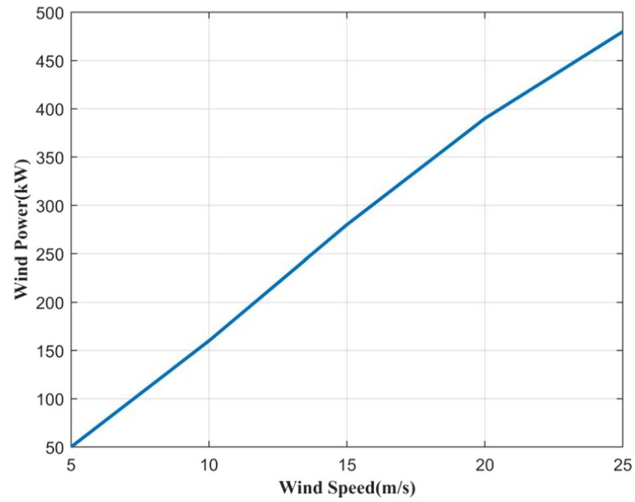

Fig. 7 Analysis of power generated by the wind regarding the wind speed

Result and Discussion

Here, the proposed HPGS's performance is evaluated. The proposed methodology is executed in MATLAB/SIMULINK. Figure 4 exhibits the proposed model's simulation diagram.

The proposed model's Simulink output is represented in Fig. 4. To glean the wind's kinetic energy, the WTs utilize the blades; moreover, the kinetic energy is transmuted into mechanical power by the WTs. To produce hot gas, the biomass is burned in the combustor; then, to produce steam, the obtained gas is inputted into the boiler.Then, via the steam turbine, it is extended to engender mechanical energy. Alternating Current (AC) is transmuted into Direct Current (DC) by the three-phase bridge rectifier. Eventually, to ameliorate the hybrid power generator, the proposed ASS-MPPT-TTSO is utilized.

Performance Analysis

Here, the proposed model's performance is evaluated. The tables, as well as the figures given below, show the analyses.

The wind speed with respect to the month from January to December is represented in Table 1. Here, the speed of the wind achieves above 3 m/s during the month. Among all these months, during March, the wind speed was high, which achieved 3.8527, followed by 3.7926 during April. During the month of September and October, the wind speed

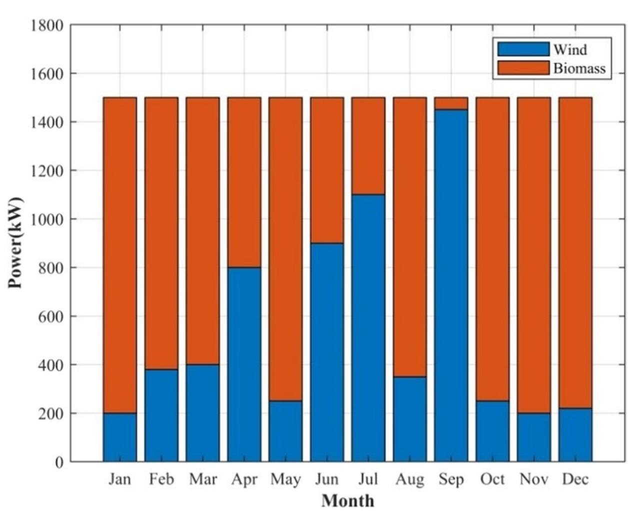

Fig. 6 Graphical representation of the generation of power during various months

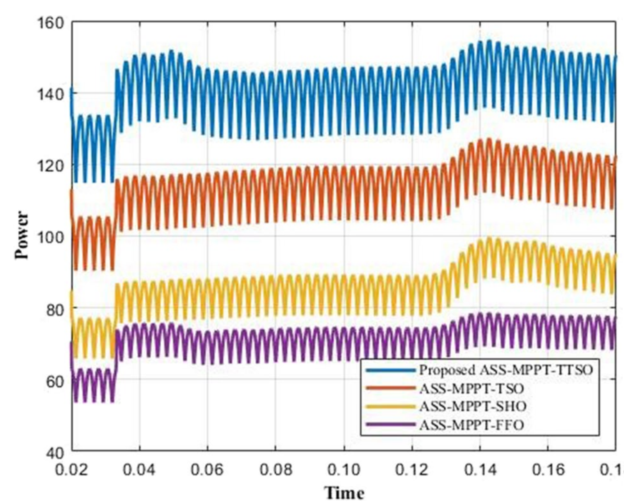

Fig. 8 Comparison of proposed ASS-MPPT-TTSO with other existing methods of ASS-MPPT-TSO, ASS-MPPT-SHO, and ASS-MPPT-FFO for power generation

Table 3 Maximum and minimum power output analysis

Methods	Output power Maximum	Output power Minimum
Proposed ASS-MPPT-TTSO	154.7175	114.78
ASS-MPPT-TSO	127.32	90.28
ASS-MPPT-SHO	99.68	65.7
ASS-MPPT-FFO	78.66	53.54

was low. Figure 5 shows the graphical representation for the analysis of the wind speed during various months.

The analysis of wind and biomass power produced from January to December is demonstrated in Table 2. Here, during September, the wind power produced is high, which is 1450 kW power; then, in September, the biomass produced 50 kW power; when analogized will all the months, lesser power is formed in September followed by July and June. In both January and November, the biomass power was high, which is 1300 kW power, and the wind-generated 200 kW power. The second-highest number of biomass power produced in December is 1280 kW power followed by May and October (1250 kW), August (1150 kW), and so on. Additionally, Fig. 6 displays the graphical representation.

The analysis of wind power regarding wind speed is shown in Fig. 7. Here, the wind speed values are measured from 5 m/s to 25 m/s; in addition, the wind power values range from 50 to 500 kW power. Regarding the wind speed, the wind speed was increased constantly; moreover, the wind power generated approximately 480 kW power at 25 m/s of wind speed.

Comparative Analysis

Here, ASS-MPPT Tunicate Swarm Optimization (ASS-MPPT-TSO), ASS-MPPT Spotted Hyena Optimizer (ASS-MPPT-SHO), and ASS-MPPT Fruit Fly Optimizer (ASS-MPPT-FFO) are the prevailing methodologies with which the proposed ASS-MPPT-TTSO is compared. The comparison is done by power with respect to time. In Fig. 8, the proposed methodology's performance is compared with other prevailing methodologies.

Table 4 Life cycle Cost Analysis with respect to energy

Wind/Biomass (KW)	Life Cycle Cost (in Lakhs)
0.2	25.13
0.4	25.22
0.6	25.67
0.8	25.92
1	26.01

The proposed model analogized with other prevailing methodologies like ASS-MPPT-TSO, ASS-MPPT-SHO, and ASS-MPPT-FFO is shown in Fig. 8. Here, the range of time is from 0.02 to 0.10 s. All the methodologies achieve higher power when the time is in 0.08 s; moreover, among these methodologies, the proposed ASS-MPPT-TTSO achieves nearly 160 kW; conversely, the other prevailing methodologies like ASS-MPPT-TSO achieve nearly 130 kW power, ASS-MPPT-SHO achieves 100 kW power and ASS-MPPT-FFO achieves below 80 kW power. When analogized with all the methodologies, the proposed ASS-MPPT-TTSO method achieves higher power. Therefore, it is evident that a better result is achieved by the proposed methodology than the prevailing algorithms.

The maximum, as well as minimum power attained by the proposed and several prevailing methodologies, is analyzed in Table 3. From Table 3, the proposed model's maximum power output is 154.7175 KW, which is higher than the conventional methodologies. In the same way, the proposed ASS-MPPT-TTSO's minimum power output is 114.78 KW. Figure 9 exhibits the graphical representation of the proposed ASS-MPPT-TTSO and the prevailing ASS-MPPT-TSO, ASS-MPPT-SHO, and ASS-MPPT-FFO methodologies.

The graphical representation of the proposed ASS-MPPT-TTSO analogized with the prevailing methodologies like ASS-MPPT-TSO, ASS-MPPT-SHO, and ASS-MPPT-FFO is shown in Fig. 9. The proposed graphical methodology was displayed based on power, voltage, input current, and three-phase rectifier. For high-power applications, the three-phase rectifier was utilized since it has a higher power utilization factor for the three-phase system. To create a wave, the diodes, transistors, thyristors, or converters were utilized by the three-phase rectification. In Fig. 9(a), regarding the time ranges from 0.02 s to 0.04 s, the power generation constantly increases from 140 to 150 kW. The given supply voltage was low within the given respective time between 0.02 to 0.04; alternatively, the supply voltage values differ as of high to low or low to high with other time ranges. The current of a three-phase rectifier input waveform was represented in various ways and the rectified output was also displayed ranging from above –20A to above 20A. To measure a voltage, the sinusoidal wave of a three-phase rectifier was activated. The voltage ranges from -100 V to 100 V. Figure 9(b) represents the conventional methodology of ASS-MPPT-TSO; in this, the power increases by nearly 130 kW regarding the time of 0.14 s to 0.16 s; in addition, the given supply voltage was also increased betwixt these periods by achieving 1320 V. Next, the input current waveform's three-phase rectifier was displayed where the value ranges from above -20A to above 20A; similarly, the sinusoidal wave represented the

Fig. 9 Graphical representation of (**a**) proposed ASS-MPPT-TTSO, (**b**) ASS-MPPT-TSO, (**c**) ASS-MPPT-SHO, and (**d**) ASS-MPPT-FFO

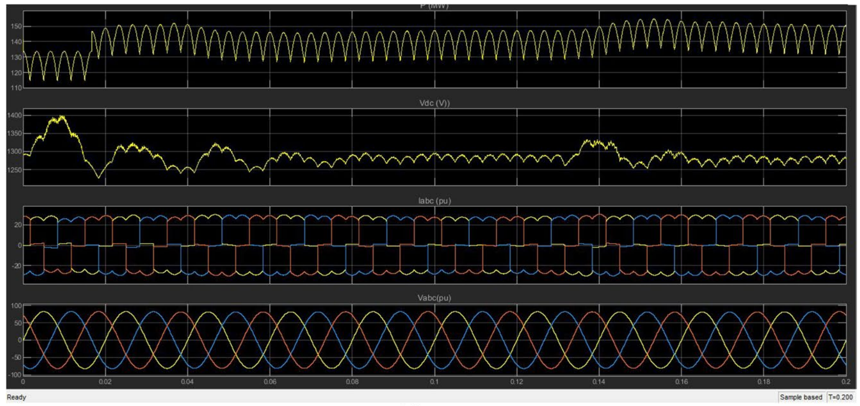

(a)

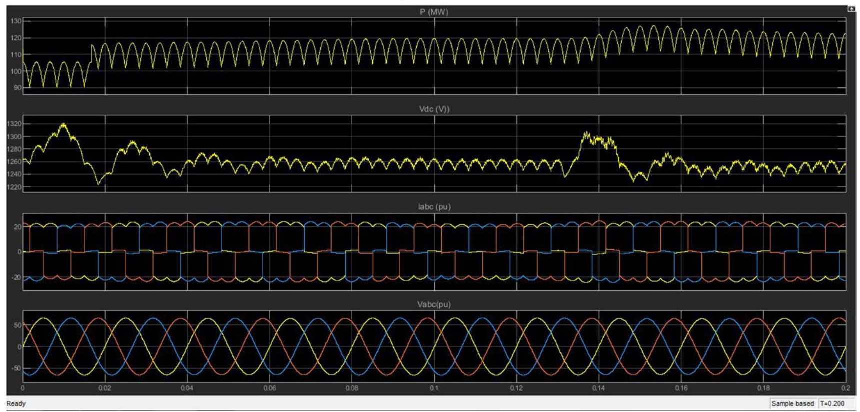

(b)

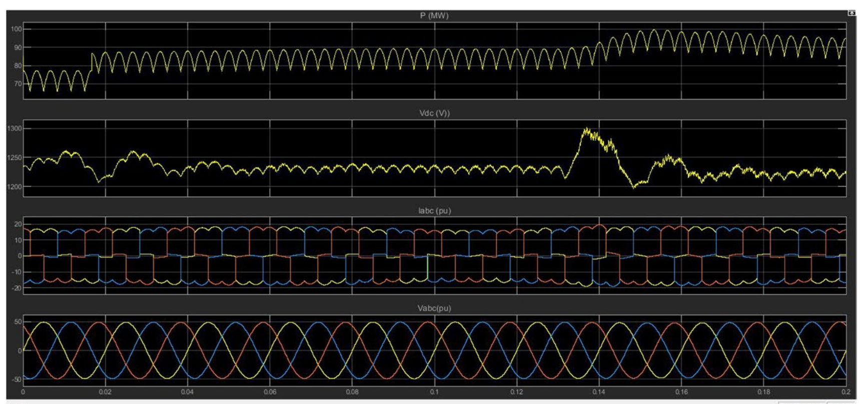

(c)

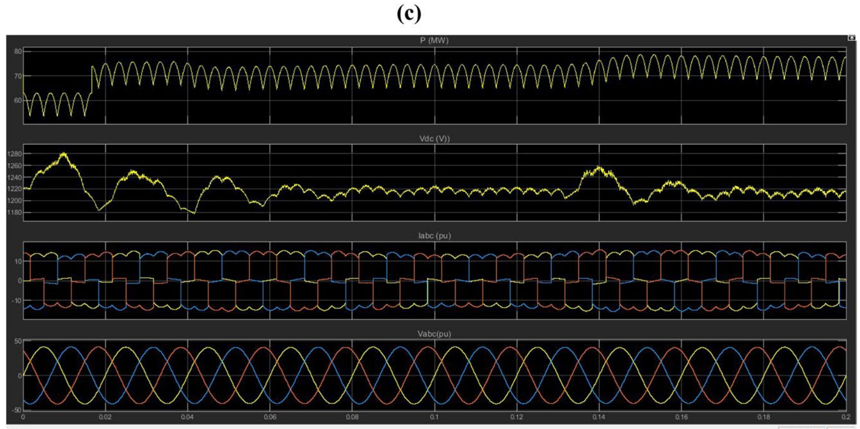

(d)

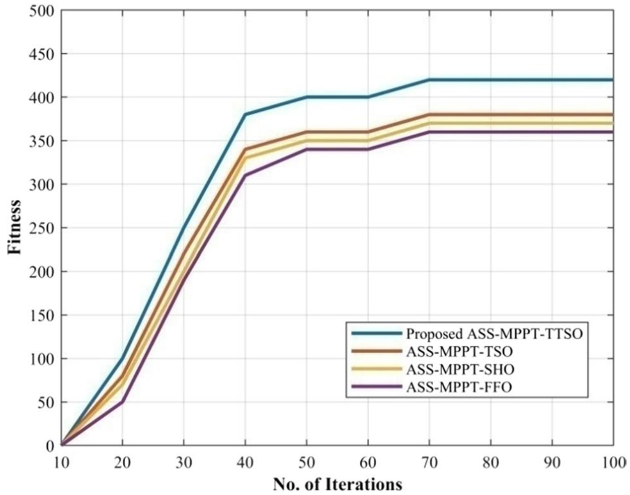

Fig. 10 Graphical representation of Fitness vs. iteration analysis

voltage of a three-phase rectifier where the value ranges from -50 V to 50 V. Figure 9 (c) shows the analysis of the prevailing ASS-MPPT-SHO model. Here, the power highly increased from 0.14 s to 0.16, which generated power of nearly 100 kW, and the supply voltage was increased above 1300 V with the given respect time from 0.12 s to 0.14 s. Then, the three-phase rectifier's current input was displayed. The given output exhibits that the current waveform was represented betwixt less than -20A to less than 20A, and the sinusoidal wave was also displayed, which ranges from -50A to 50A. The prevailing methodology of ASS-MPPT-FFO was analyzed in Fig. 9 (d). The high power generated was nearly 80 kW power from 0.14 s to 0.18 s. Betwixt 0–0.02 s, the supply voltage produced higher voltage; in addition, achieved nearly 1280 V. The three-phase rectifier of a current waveform and sinusoidal waveform of a voltage was displayed; subsequently, the current waveform ranges from above -10A to above 10A, and the sinusoidal ranges from -50 V to 50 V. By giving a higher power, the proposed methodology delivers better performance than the other prevailing methodologies. The proposed ASS-MPPT-TTSO achieves power from 140–150 kW; conversely, the other methodologies achieved nearly 130 kW, 100 kW, and below 80 kW. Therefore, the proposed methodology provides better performance than the prevailing methodologies.

Regarding the number of iterations, the fitness function of the proposed ASS-MPPT-TSO methodology is analyzed with the other prevailing methodologies like ASS-MPPT-TSO, ASS-MPPT-SHO, and ASS-MPPT-FFO in Fig. 10. Here, for the analysis, 10 to 100 iterations were taken. The proposed ASS-MPPT-TTSO's fitness function is approximately 430 for a count of 100. In the same iteration, the prevailing ASS-MPPT-TSO, ASS-MPPT-SHO, and ASS-MPPT-FFO achieved nearly 380, 370, and 360 fitness

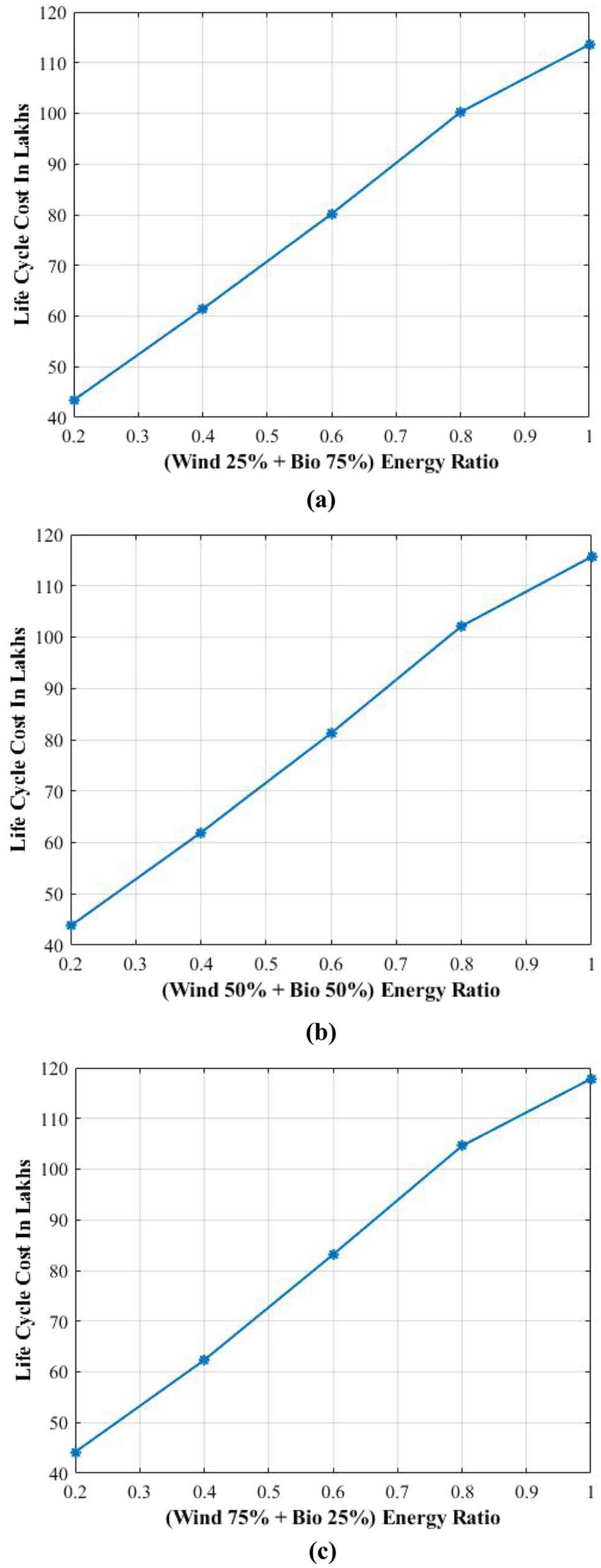

Fig. 11 Lifecycle cost analysis under three cases (**a**) 25% wind-75% biomass (**b**) 50% wind-50% biomass (**c**) 75% wind-25% biomass

functions. Here, the highest fitness function was achieved by the proposed AS-MPPT-TTSO, and the lowest fitness function was achieved by the ASS-MPPT-FFO. Similarly, the proposed model has better fitness outcomes than the prevailing methodologies for the remaining iteration count also. Consequently, it is evident that a better outcome was achieved by the proposed model than the prevailing methodologies.

The wind-biomass hybrid system's life cycle cost was analyzed in Table 4 regarding the energy ratio varying from 0.2 to 1. Here, a lower life cycle cost of 25.13 lakhs was attained by the model when the ratio is 0.2 (8 KW of wind and 32 KW of biomass). For the energy ratio of 1, the model shows a higher lifecycle cost of 26.01 lakhs.

The variation of lifecycle cost for different proportions of the wind-biomass hybrid system is exhibited in Fig. 11. (a) 25% wind-75% biomass, (b) 50% wind-50% biomass, and (c) 75% wind-25% biomass are the proportions deemed for the evaluation. Amongst all these, the maximum life cycle cost is possessed by the HES with a ratio of 75% wind and 25% biomass. It reveals that the model's life cycle cost increases as the biomass energy proportion decreases.

Conclusion

Here, a framework for an HPGS has been proposed with a three-phase bridge rectifier along with an inverter. Here, to regulate the output voltage, an ASS-MPPT is utilized with a Perturb and Observe technique for inverter control. Thus, the proposed model's robustness along with efficacy is enhanced considerably. Next, to validate the proposed system's effectiveness, the experimental evaluation is conducted; in this, regarding certain performance metrics, the performance along with comparative analysis is performed. The final result shows that with an output power of 160 kW, higher efficiency was attained by the proposed methodology. On the whole, the proposed model remains more reliable and robust by outperforming the prevailing methodologies. In the future, with some enhanced methodologies, the work will be extended; furthermore, the power generation system's efficacy could be ameliorated.

Authors' Contributions All author is contributed to the design and methodology of this study, the assessment of the outcomes and the writing of the manuscript.

Funding Authors did not receive any funding.

Data Availability No datasets were generated or analyzed during the current study.

Code Availability Not applicable.

Declarations

Conflicts of Interests Authors do not have any conflicts.

References

1. Aziz MS, Ahmed S, Saleem U, Mufti GM (2017) Wind hybrid power generation systems using renewable energy sources a review. Int J Renew Energy Res 7(1):1–18
2. Bhattacharjee S, Nandi C (2020) Design of a voting based smart energy management system of the renewable energy based hybrid energy system for a small community. Energy 214:1–40
3. Mahto T, Malik H, Mukherjee V (2019) Fractional order control and simulation of wind biomass isolated hybrid power system using particle swarm optimization. In: Advances in Intelligent System and Computing, 1st edn., vol 1. Springer, Singapore. https://doi.org/10.1007/978-981-13-1819-1_27
4. Bhattacharjee S, Chakraborty S, Jena BB, Deb S, Das R (2018) An optimization study of both on-grid and off- grid solar-wind-biomass hybrid power plant in Nakalawaka, Fiji. Int J Res Appl Sci Eng Technol 6(4):3823–3834
5. Mohammed Abdali AL, Yakimovich BA, Kuvshinov VV (2019) Hybrid power generation by using solar and wind energy. World J Mech 9(4):81–93
6. Karsh RK, Debnath R, Soren N, Roy AK, Pandey AD (2019) Optimal Economical analysis and performance assessment of wind-biomass hybrid energy system. International Conference on Automation, Computational and Technology Management, 24–26 April 2019, London, UK. https://doi.org/10.1109/ICACTM.2019.8776854
7. Sahoo U, Kumar R, Pant PC, Chaudhary R (2017) Development of an innovative polygeneration process in hybrid solar biomass system for combined power, cooling and desalination. Appl Thermal Eng 120:560–567
8. Tajeddin A, Roohi E (2019) Designing a reliable wind farm through hybridization with biomass energy. Appl Thermal Eng 154:171–2179
9. Suresh V, Muralidhar M, Kiranmayi R (2020) Modelling and optimization of an off-grid hybrid renewable energy system for electrification in a rural areas. Energy Reports 6:594–604
10. Ahmad J, Imran M, Khalid A, Iqbal W, Ashraf SR, Adnan M, Ali SF, Khokhar KS (2018) Techno economic analysis of a wind photovoltaic biomass hybrid renewable energy system for rural electrification a case study of KallarKahar. Energy 148:208–234
11. Chowdhury T, Chowdhury H, Miskat MI, Chowdhury P, Sait SM, Thirugnanasambandam M, Saidur R (2019) Developing and evaluating a stand-alone hybrid energy system for Rohingya refugee community in Bangladesh. Energy 191:1–46
12. Li J, Liu P, Li Z (2020) Optimal design and techno economic analysis of a solar wind biomass off-grid hybrid power system for remote rural electrification a case study of west China. Energy 208:1–33
13. Wang Y, Lou S, Yaowu Wu, Miao M, Wang S (2019) Operation strategy of a hybrid solar and biomass power plant in the electricity markets. Electric Power Syst Res 167:183–191
14. Kumar V, Ghosh S, Naidu NKS, Kamal S, Saket RK, Nagar SK (2021) Load voltage based MPPT technique for standalone PV systems using adaptive step". Int J Electr Power Energy Syst 128:1–11
15. Chowdhury N, Hossain CA, Longo M, Yaïci W (2020) Feasibility and cost analysis of photovoltaic-biomass hybrid energy system in off-grid areas of Bangladesh. Sustainability 12(4):1–15

16. Alturki FA, Al-Shammaa AA, Farh HMH, AlSharabi K (2020) Optimal sizing of autonomous hybrid energy system using supply-demand-based optimization algorithm. Int J Energy Res 1:1–21
17. Paliwal NK, Singh AK, Singh NK, Kumar P (2018) Optimal sizing and operation of battery storage for economic operation of hybrid power system using artificial bee colony algorithm. Int Trans Electr Energy Syst 29(5):1–23
18. Berbaoui B, Dehini R, Hatti M (2019) An applied methodology for optimal sizing and placement of hybrid power source in remote area of South Algeria. Renewable Energy 146:1–25
19. Dinga Z, Houa H, Yua G, Hub E, Duana L, Zhao J (2019) Performance analysis of a wind-solar hybrid power generation system. Energy Convers Manag 181:223–234
20. Ji L, Liang X, Xie Y, Huang G, Wang B (2021) Optimal design and sensitivity analysis of the stand-alone hybrid energy system with PV and biomass CHP for remote villages. Energy 225(3):1–16
21. El-Houari H, Allouhi A, Rehman S, Buker MS, Kousksou T, Jamil A, El Amrani B (2020) Feasibility evaluation of a Hybrid Renewable Power Generation System for sustainable electricity supply in a Moroccan remote site. J Clean Prod 277:1–52
22. Jahangir MH, Cheraghi R (2020) Economic and environmental assessment of solar wind biomass hybrid renewable energy system supplying rural settlement load. Sustain Energy Technol Assess 42:1–14
23. Al-Ghussain L, Ahmad AD, Abubaker AM, Mohamed MA (2021) An integrated photovoltaic wind biomass and hybrid energy storage systems towards 100% renewable energy microgrids in university campuses. Sustain Energy Technol Assess 46(1):1–13
24. Shezan SKA, Ping HW (2017) Techno economic and feasibility analysis of a hybrid PV-wind-biomass- diesel energy system for sustainable development at offshore areas in Bangladesh. Current Alternative Energy 1(1):20–32
25. Lee J-Y, Aviso K, Tan RR (2018) Optimal sizing and design of hybrid power systems. ACS Sustain Chem Eng 6(2):2482–2490